

Adaptive Soft Sensing and On-line Estimation of the Critical Minimum Velocity with Application to an Oil Sand Primary Separation Vessel^{*}

Nima Sammaknejad, Biao Huang¹, R. Sean Sanders, Yu Miao^{*}
Fangwei Xu, Aris Espejo^{**}

^{*} Department of Chemical and Materials Engineering, University of Alberta, Edmonton, Alberta, Canada T6G 2V4

^{**} Syncrude Canada Ltd., Fort McMurray, Alberta, Canada T9H 3L1

Abstract: Most of the previous studies on the required critical minimum velocity to move the solid bed inside the slurry pipelines are related to the design step where the dynamics of the process are not thoroughly considered. In this paper, a general framework for on-line estimation of the critical minimum velocity is proposed and applied to the underflow stream of an important Primary Separation Vessel (PSV) in an oil sand industry. Appropriate statistical and probabilistic models are used to improve the on-line measurements and estimations. The proposed method demonstrates a satisfactory performance in detection of different conditions of the PSV operations.

Keywords: Fault detection, Critical minimum velocity estimation, Soft sensing, Probabilistic models, Oil sand industry.

1. INTRODUCTION

1.1 Process Overview

The industrial application of this paper is critical minimum velocity estimation in the underflow pipeline of an industrial scale PSV in oil sand industry. The PSV unit is schematically presented in Fig. 1.

The PSV unit is a large settling vessel to separate the feed into three different streams. The slurry feed, which includes aerated bitumen aggregates, water, coarse sand and fine solids, enters at the center of the unit. The bitumen floats over a weir circling the top for further froth treatment. Coarse sand particles settle to the bottom and form the underflow stream. A third outlet stream, which usually contains fines, bitumen aggregates and water, is removed from the middle of the vessel and referred to as middlings. Both middlings and underflow streams are transferred to secondary recovery units with limited recovery rate by using two variable speed pumps through two different pipelines.

1.2 Definition of the Critical Minimum Velocity

The critical minimum velocity, also known as the deposition velocity, is the operational velocity at which the stationary bed of solids first forms. The diagram of the

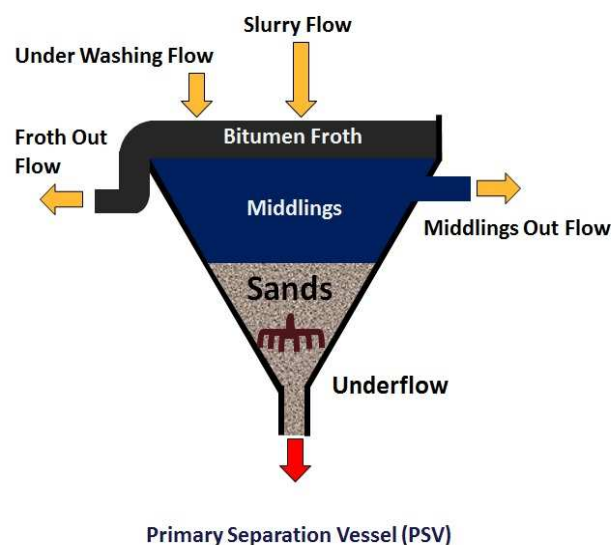


Fig. 1. Three layers of the PSV unit

pressure loss inside the pipeline ($\frac{Pa}{m}$) versus average mixture velocity ($\frac{m}{s}$) for water and the slurry flow is available in literature (Poloski et al. (2009)).

In the case of having water inside the pipeline, the pressure loss increases while raising the average mixture velocity. However, in the case of slurry flow, there is a velocity below which the particles start to make a stationary bed, and right above it, the bed of particles starts to move. This critical point, where the pressure loss inside the slurry

^{*} The authors would like to acknowledge financial support from NSERC and Syncrude Canada Ltd.

¹ Corresponding author. Tel:+1 780 492-9016, Fax: +1 780 492-2881, E-mail address: biao.huang@ualberta.ca

pipeline becomes the minimum, is known as the critical minimum velocity or the deposition velocity.

1.3 Importance of the Critical Minimum Velocity

Since the underflow stream in the PSV unit usually contains coarse sand particles, there is a concern of sand deposition and pipeline plugging. Complete plugging of the pipeline, which occurs at flow-rates below the critical velocity, is referred to as the “sanding” phenomena in oil sand industry. In addition to the sanding phenomena, operating velocities below the critical minimum velocity will cause excessive erosion in the lower part of the pipeline (Lahiri et al. (2010)).

On the other hand, operating velocities greater than the critical minimum velocity are uneconomical as more pump power will be required (Lahiri et al. (2010)).

On-line estimation of the critical minimum velocity and comparison with the current operating velocity will provide a lower limit for the operator to avoid near sanding as well as sanding regions. Also, it will help to avoid conservative high flow-rate operations in the underflow stream, and therefore, improve PSV bitumen recovery.

1.4 Solution Strategy

Unlike the previous applications where the critical minimum velocity equations are only used in the design step, in this paper, a novel approach for on-line estimation of the critical minimum velocity with application to the underflow stream of the PSV unit is introduced. When the on-line estimation becomes greater than the current operating velocity, a near-sanding alarm is generated.

The solution strategy is as follows:

First, the appropriate semi-empirical equation for on-line estimation of the critical minimum velocity is selected. Next, the effective variables for the estimation are obtained. Since one of the key variables, carrier fluid density, has some inaccurate on-line measurement, a soft sensor is developed to provide a parallel on-line measurement for this variable. The recursive Partial Least Squares (rPLS) method is used to develop this soft sensor. Also, an adaptive approach based on Hidden Markov Models (HMMs) is used to adaptively change the sensitivity of the critical velocity estimations. Due to the presence of unknown operating modes, the Expectation Maximization (EM) algorithm is used to train the HMM. Finally, the algorithm is tested in on-line environment through the connection to the Distributed Control System (DCS), OPC server and MATLAB.

2. CRITICAL MINIMUM VELOCITY ESTIMATION

Numerous semi-empirical equations have been developed for the purpose of deposition velocity estimation in literature (Durand (1953) and Turian et al. (1987)). They are based on both force balance and laboratory analysis. Quality of these models depends primarily on the quality of the experimental data.

As explained by Poloski et al. (2009), Shook et al. developed a correlation between the Archimedes (Ar) and Froude (Fr) numbers to estimate the critical minimum

velocity. Shook et al. introduce the Archimedes number as an independent variable and provide the following relation between the Archimedes and Froude numbers (Gillies et al. (2000), Shook et al. (2002)):

$$\begin{aligned} 540 < Ar, Fr &= 1.78Ar^{-0.019} \\ 160 < Ar < 540, Fr &= 1.19Ar^{0.045} \\ 80 < Ar < 160, Fr &= 0.197Ar^{0.4} \end{aligned} \quad (1)$$

This equation, which is known as the SRC (Saskatchewan Research Council) equation, is based on a large data-base with properties similar to the underflow pipeline of the PSV unit. It is developed based on high quality experimental data and is applicable to the turbulent flows and a variety of pipeline diameters from 0.05 to 0.5 [m]. Combination of all these properties makes the SRC equation an appropriate choice for the industrial application of this paper.

The key variables for estimation of the critical minimum velocity using the SRC equation are as follows:

2.1 Carrier Fluid Density (ρ_f)

Carrier fluid is a portion of the slurry which contains fine and particles with diameter less than 44 [μm] (Shahmirzad (2012)). In the PSV unit, as presented in Fig. 1, coarser particles usually settle to the tailings stream while fines and bitumen aggregates enter the middlings stream. Therefore, the middlings stream provides a good indication to the carrier fluid properties. In this study, middlings density, which is measured through an on-line analyzer, is used as an indication to the carrier fluid density in the SRC equation.

2.2 Carrier Fluid Viscosity (μ_f)

Carrier fluid viscosity is known to be a function of carrier fluid solid concentration in fluid particle systems literature. Having the value of the carrier fluid density as explained in the previous section, the carrier fluid solid concentration can be obtained from (2):

$$\rho_f = C_f \rho_s + (1 - C_f) \rho_l(T) \quad (2)$$

where C_f is the carrier fluid solid concentration, ρ_s is the density of the solid phase, which is often selected as 2650 [$\frac{kg}{m^3}$] in oil sand industry as an average, and $\rho_l(T)$ is the density of the liquid phase (water is the dominant component) as a function of the PSV temperature (T) from Tanaka's equation (Tanaka et al. (2001)).

Having the carrier fluid solid concentration, various semi-empirical correlations exist in literature to find the carrier fluid viscosity. Among them, our investigation on the historical data of the PSV shows that Equation (3), which is developed in conditions close to the middlings stream (Smith (2013)), is appropriate for this industrial case study. The linear behavior of this equation provides smooth estimations for the critical minimum velocity.

$$\mu_f = \mu_l(T)(1 + 14.7C_f) \quad (3)$$

where $\mu_l(T)$ is the viscosity of the liquid phase (water is the dominant component) as a function of temperature (T) in Kelvin. This equation is explained in detail in literature (Al-Shemmeri (2012)).

2.3 Coarse Particle Diameter

Coarse particle diameter plays an important role in estimation of the critical minimum velocity. Intuitively, coarse particle diameter should have a positive correlation with the ratio of volumetric concentration of coarse solids to fines in the mixture as in (4). Similar intuitive correlations are available in literature (Brown (2003)).

$$d \propto X = \frac{C_{mix} - C_{fines}}{C_{fines}} \quad (4)$$

where d is the coarse particle diameter, C_{mix} is the volumetric concentration of solids in the mixture and C_{fines} is the volumetric concentration of fines in the mixture.

In (4), one could see that in the case of having no coarse particles in the mixture ($C_{mix} = C_{fines}$), the X factor becomes zero. When the ratio of $(\frac{C_{mix}}{C_{fines}})$ starts to increase, i.e., there are more coarse particles in the mixture, the X factor starts to grow. Since d is the median of all available particle diameters in the mixture, it is expected to have a positive correlation with the X factor. As previously stated in the introduction section, fines and bitumen aggregates usually enter the middlings stream while the coarser particles tend to go directly to the tailings. Therefore, the X factor in (4) can be written as,

$$X = \frac{C_{und} - C_{mid}}{C_{mid}} \quad (5)$$

where "und" and "mid" refer to underflow and middlings streams respectively.

In this study, the positive correlation between coarse particle diameter and the X factor is assumed to be linear. More complicated correlations can be considered as a subject of future studies. Having the minimum and maximum value of the coarse particle diameter (Sanders et al. (2000)), the minimum and maximum value of the X factor from historical data, and the linearity assumption, the on-line estimation of coarse particle diameter can be calculated as in (6):

$$\frac{X - X_{min}}{X_{max} - X_{min}} = \frac{d - d_{min}}{d_{max} - d_{min}} \quad (6)$$

Since this equation is subject to many uncertainties, it is only applied when the X factor is within two standard deviations of X_{mean} . Otherwise the coarse particle diameter is assumed to be constant (d_{mean}).

3. SOFT SENSOR DEVELOPMENT

From the previous sections, one could observe that carrier fluid density, which is available through middlings density analyzer, plays a key role in on-line estimation of the critical minimum velocity. However, there are several

short periods in the historical data where this on-line measurement is not available. Maintenance of the PSV or exceeding the measurement limits is the main reason of such circumstances. During such periods, the data which appears in DCS represents the lower limit of the online analyzer, and not the true value. As a result of such malfunctions, the Archimedes number suddenly decreases. This results in a sudden spike, and a false alarm in on-line estimation of the critical minimum velocity.

Consequently, providing another on-line measurement parallel to the density on-line analyzer will help to avoid such false alarms and malfunctions in the case of on-line analyzer failure (see Fig. 4 and Fig. 5 for more information). Lab data for the middlings density is available every two hours.

Density of the middlings stream is strongly correlated with the density of other layers, e.g., feed, froth and the underflow. Therefore, linear regression techniques like Partial Least Squares (PLS) provide appropriate data-driven models to solve this problem. However, since the PSV unit shows a time varying behavior according to the historical data (working conditions of the PSV might change due to the changes in the feed properties) model updating is necessary.

3.1 Recursive Exponentially Weighted PLS (rPLS)

Many different approaches have been reported in literature in order to update the model in the on-line application. One of the simplest ways is known as model coefficients recalculation (Li et al. (2010)). Such methods will cause some delay in model updating. Successful applications of the recursive Partial Least Squares (rPLS) method in industrial processes are reported in literature (Haavisto et al. (2009)). Unlike the model coefficients recalculation methods, the rPLS method significantly weights every new sample to the data-base and continuously updates the model. Therefore, the model will more rapidly adapt to new process conditions.

The rPLS method used in this paper is based on the study on improved PLS kernel algorithm by Dayal et al. (1997-A). In this updating strategy, a forgetting factor is used to exponentially discount the past data and takes into account the effect of the recent observations (Dayal et al. (1997-B)). The covariance matrix is updated as follows (Chen (2013)):

$$\begin{aligned} R_{xx}(t) &= \lambda R_{xx}(t-1) + \tilde{x}(t)^T \tilde{x}(t) \\ R_{xy}(t) &= \lambda R_{xy}(t-1) + \tilde{x}(t)^T \tilde{y}(t) \end{aligned} \quad (7)$$

where the forgetting factor ($0 \leq \lambda \leq 1$) reflects the rate of discounting the old data. The procedure to update the mean centered data ($\tilde{x}(t)$ and $\tilde{y}(t)$) for the new available inputs and outputs is explained in detail in literature (Chen (2013)).

When the new covariance matrices are available from (7), the regression coefficients (b) are obtained following a fast kernel PLS calculation. Details of the method can be found in Dayal et al. (1997-A). Having the regression coefficients available, the mean centered final prediction (\hat{y}_t) in on-line application is obtained as,

$$\hat{y}_t = bX_t \quad (8)$$

where X_t is the mean centered vector of input variables at time t .

Results of the rPLS algorithm will be compared to the fixed PLS in the Results Section.

4. ADAPTIVE SENSITIVITY LEVELS FOR CRITICAL VELOCITY ESTIMATION

The main idea of the work presented in this section is to adaptively change the sensitivity of the critical velocity estimations according to the operating mode of the process. Consequently, more sensitive predictions will be generated when the process is operating more abnormally and the prediction sensitivity decreases when the process is in normal operating condition.

In order to avoid false alarms and provide more sensitive predictions, it is necessary to adaptively select the $K(t)$ value in (9).

$$Q_S(t) = Q_C(t) + K(t) \times \sigma_{Q_C} \quad (9)$$

where $Q_S(t)$ is the sensitive estimation of $Q_C(t)$ (critical flow-rate) based on the current operating mode of the real flow-rate at time t (F_t), and σ_{Q_C} is the standard deviation of the critical flow-rate estimation error due to the midlings density measurement errors, which is obtained from a Monte-Carlo simulation. Note that, having the diameter of the pipeline, velocity can be easily converted to flow-rate.

The lower and upper bounds of the K value ($K_{L/U}$) in (9) can be obtained by solving the optimization problem in (10) based on different sensitivity values, e.g., use $\alpha_L = 0.7$ to find K_L and $\alpha_U = 1$ to find K_U , etc.

$$K_{L/U} = \operatorname{argmin}_K \|Q_S - \alpha_{L/U} F_{Normal}\| \quad (10)$$

where F_{Normal} is the vector of normal flow-rates of the process from historical data.

The historical data for the underflow flow-rate can be divided to three operating modes (I_t 's), i.e., mode 1 ($I_t = 1$) is low flow rate, mode 2 ($I_t = 2$) is average flow rate and mode 3 ($I_t = 3$) is the high flow-rate. In the application of this paper, mode 1 (near sand deposition and plugging) and mode 3 (impact on the bitumen recovery) are considered as upset operations. In order to avoid such regions, the $K(t)$ value will be adaptively selected according to (11):

$$\frac{K(t) - K_L}{K_U - K_L} = 1 - P(I_t = 2 | F_t, \dots, F_0) = P(\text{Upset Modes}) \quad (11)$$

where F_t, \dots, F_0 are the underflow flow-rate observations from time 0 to t , and $P(\text{Upset Modes})$ is the probability of the upset operating modes to occur.

Adaptive selection of the K value according to (11) will increase the sensitivity of the estimations in the upset operating modes, while reducing the sensitivity in the normal modes. Using this adaptive technique, the number of false alarms will be greatly reduced.

4.1 Flow-rate Mode Diagnosis

In order to calculate $P(I_t | F_t, \dots, F_0)$ in (11), Hamilton's filtering strategy is used to infer the operating mode of the process (Hamilton (1988)). It is assumed that operating modes of the flow-rate can transit to each other following a Markov chain model with mean values, variances, state transition probabilities and initial state distributions given as $\mu_i, \sigma_i^2, \alpha_{ij}$ and π_i where i and j ($1 \leq i, j \leq M = 3$) are indicators of the operating mode ($I_t = i, j, 1 \leq i, j \leq M$). The training procedure to obtain these parameters will be explained in the next section. More details regarding this filtering strategy for an online diagnosis application is available in literature (Hamilton (1988)).

4.2 HMM Training

In this section, the procedure of training HMMs to model the transitions of the flow-rate is introduced. Following the proposed strategy of this section, means and variances of the different operating modes of the flow-rate (μ_i 's and σ_i^2 's), the transition probabilities (α_{ij} 's) and initial state distribution of the Markov chain model (π) will be obtained.

Due to the existence of the unknown operating modes, the Expectation Maximization (EM) algorithm provides appropriate solutions to this problem. The training procedure of this paper is adopted from the study by Hamilton (1990). Our recent studies provide a more general solution to such problems in the presence of both continuous and discrete observations (Sammaknejad et al. (2014), and Sammaknejad et al. (2015)).

Means, variances, transition probabilities and the initial state distributions can be found from the update equations (12) to (15) respectively.

$$\mu_i^{(n)} = \frac{\sum_{t=1}^N F_t P(I_t = i | \theta^{(n-1)}, C_{obs})}{\sum_{t=1}^N P(I_t = i | \theta^{(n-1)}, C_{obs})} \quad (12)$$

where $\theta^{n-1} = \{\mu_i^{n-1}, \sigma_i^{n-1}, \alpha_{i,j}^{n-1}, \pi_i^{n-1}\}, 1 \leq i, j \leq M$, is the set of parameters from the previous iteration starting from the initial value θ^0 , and $C_{obs} = \{F_1, \dots, F_N\}$ is the set of observations in the training data-set with length N . n is an indicator of the iteration number.

$$(\sigma_i^{(n)})^2 = \frac{\sum_{t=1}^N (F_t - \mu_i^{(n)})^2 P(I_t = i | \theta^{(n-1)}, C_{obs})}{\sum_{t=1}^N P(I_t = i | \theta^{(n-1)}, C_{obs})} \quad (13)$$

$$\alpha_{ij}^{(n)} = \frac{\sum_{t=2}^N P(I_t = j, I_{t-1} = i | \theta^{(n-1)}, C_{obs})}{\sum_{j=1}^M \sum_{t=2}^N P(I_t = j, I_{t-1} = i | \theta^{(n-1)}, C_{obs})} \quad (14)$$

$$\pi_i^{(n)} = P(I_1 = i | \theta^{(n-1)}, C_{obs}) \quad (15)$$

The training procedure is iteratively repeated until certain convergence criterion is satisfied.

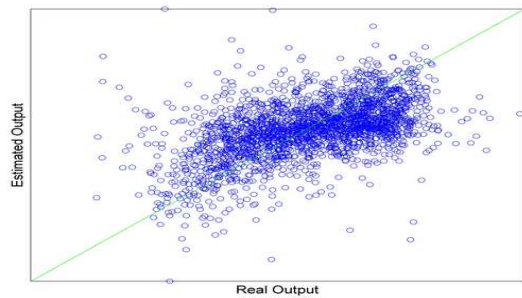


Fig. 2. Middlings density ($\frac{g}{cm^3}$) soft sensor estimations versus lab data (scatter plot)

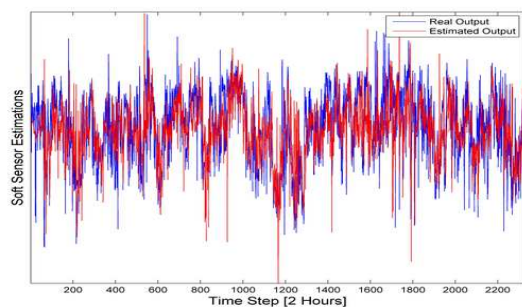


Fig. 3. Middlings density ($\frac{g}{cm^3}$) soft sensor estimations versus lab data (time trend plot)

5. RESULTS

5.1 Soft Sensor Performance

In this section, results of the middlings density soft sensor are presented. Results are compared to the soft sensor with fixed parameters (rPLS versus PLS).

Fig. 2 and Fig. 3 illustrate the results of the soft sensor predictions in 2012 historical data (scatter plot and time trend). From these figures, one could observe that the soft sensor is able to track the trend of the lab data. Comparison of the results between the fixed and recursive soft sensors is presented in Table 1. The model performance is evaluated by Root Mean Square Error of Prediction (RMSEP) and the correlation coefficient R.

Table 1. Comparison between the performance of the fixed and recursive PLS soft sensors

Soft Sensor	PLS	rPLS
RMSEP	0.2119	0.1054
R	0.4273	0.6077

The current results for the rPLS soft sensor satisfy the need to have a parallel measurement for the middlings density on-line analyzer. This parallel measurement will help to avoid false alarms and sudden spikes in the predictions of the critical velocity due to the on-line analyzer malfunctions as explained in Section 3. Fig. 4 presents a case of the on-line analyzer failure. Fig. 5 shows how the results have been improved after having a parallel measurement from the soft sensor.

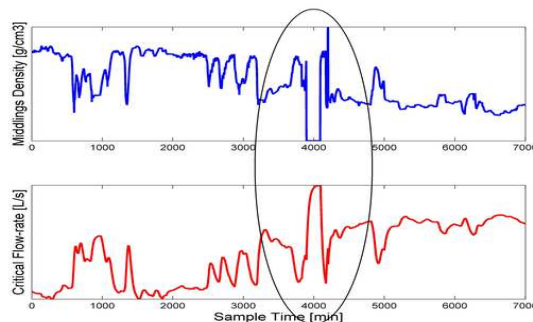


Fig. 4. Sudden spike in the prediction of the critical minimum velocity due to the on-line analyzer failure)

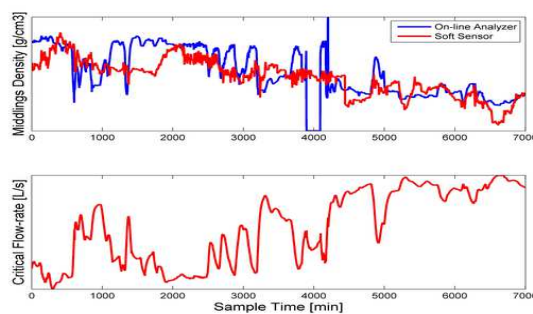


Fig. 5. Modified critical velocity estimation results in the case of analyzer failure

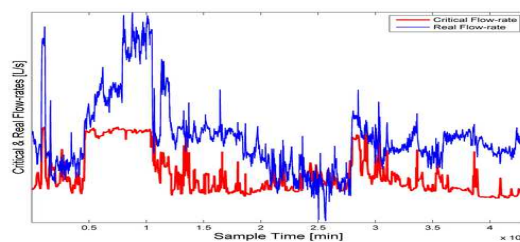


Fig. 6. A case of near sanding operation in 2013 data-set

5.2 Critical Velocity Estimation

A case of combination of normal and abnormal regions which has occurred in 2013 is presented in Fig. 6.

In this figure real (blue line) and the critical (red line) flow-rates are compared. It presents two cases of near-sanding operations which have occurred in the historical data. In both cases, the operator has increased the flow-rate to avoid sand deposition in the pipeline. However, it can be observed that in the first near-sanding operation, the flow-rate has been increased very conservatively. This might cause bitumen and energy loss in the process. Increasing velocities that are close to the critical velocity are usually sufficient to avoid near-sanding regions.

Operating modes of the flow-rate to provide critical velocity estimations with adaptive sensitivities are presented in Fig. 7.

In this figure, different operating modes of the flow-rate based on the filtering algorithm introduced in Section 4.1, and the trained Markov chain model, are presented. As previously mentioned in Section 4, and illustrated in Fig. 6,

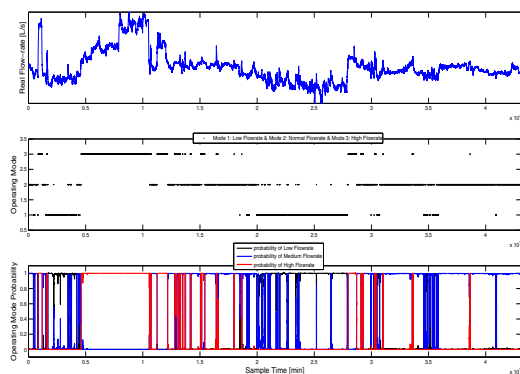


Fig. 7. Flow-rate operating modes for the data in Fig. 6
adaptive modification of estimation sensitivity based on the process operating mode will greatly reduce the number of false alarms.

6. CONCLUSION

In this paper, a novel procedure for on-line estimation of the critical minimum velocity is introduced. Application of the method is tested on the Primary Separation Vessel of an oil-sand industry. A soft sensor is developed to correct the measurements from the on-line analyzer for the key process variable. In order to reduce false alarms, an adaptive scheme based on HMMs is proposed to determine the sensitivity of the critical velocity estimations. The proposed method is tested both on-line and on the historical data of the PSV unit, and shows acceptable performance in detection of operating modes of the process. In near-sanding operating conditions, the estimated value of the critical velocity increases. A caution alarm is generated when the value of the critical velocity is higher than the current flow-rate. Increasing the underflow flow-rate by adding more water can help to return the process to the normal operating condition.

ACKNOWLEDGEMENTS

The authors would like to acknowledge financial support from NSERC and Syncrude Canada Ltd.

REFERENCES

- A.P. Poloski, H.E. Adkings, J. Abrefah, A.M. Casella, R.E. Hohimer, F. Nigl, M.J. Minette, J.J. Toth, J.M. Tingey, S.T. Yokuda. Deposition velocities of Newtonian and non-Newtonian slurries in pipelines. *PNNL-17639, WTP-RPT-175, Revision 0, Pacific Northwest National Laboratory, Richland, WA*, 2009.
- S.K. Lahiri, K.C. Ghanta. Artificial neural network model with parameter tuning assisted by genetic algorithm technique: study of critical velocity of slurry flow in pipeline. *Asia-Pacific Journal of Chemical Engineering*, 5:763-777, 2010.
- R. Durand. Basic relationships of the transportation of solids in pipes - Experimental research. *Proceedings: Minnesota International Hydraulics Convention, International Association for Hydraulic Research*, 89-103, 1953.
- R.M. Turian, F.L. HSU, T.W. MA. Estimation of the critical velocity in the pipeline flow of slurries. *Powder Technology*, 51(1):35-47, 1987.
- R.G. Gillies, J. Schaan, R.J. Sumner, M.J. McKibben, C.A. Shook. Deposition velocities for Newtonian slurries in turbulent flow. *The Canadian Journal of Chemical engineering*, 78(4):704-708, 2000.
- C.A. Shook, R.G. Gillies, R.S. Sanders. Pipeline hydrotransport with applications in oil sands industry. *SRC Pipe Flow Technology Centre*, 2002.
- A.A. Shahmirzad. The Effect of fine flocculating particles and fine inerts on carrier fluid viscosity. *MSc. Thesis, University of Alberta*, Fall 2012.
- M. Tanaka, G. Girard, R. Davis, A. Peuto, N. Bignell. Recommended table for the density of water between 0°C and 40°C based on recent experimental reports. *Metrologia*, 38:301-309, 2001.
- J.L. Smith. Measurements of carrier fluid viscosities for oil sand extraction and tailings slurries. *MSc. Thesis, University of Alberta*, Spring 2013.
- T. Al-Shemmeri. Engineering Fluid Mechanics. *Bookboon*, 2012.
- R.B. Brown. Soil Texture. *University of Florida, IFAS Extension*, 1-8, 2003.
- R.S. Sanders, A.L. Ferre, W.B. Maciejewski, R.G. Gillies, C.A. Shook. Bitumen effects on pipeline hydraulics during oil sand hydrotransport. *The Canadian Journal of Chemical Engineering*, 78(4):731-742, 2000.
- W. Li, L. Xing, L. Fang, J. Wang, H. Qu. Application of near infrared spectroscopy for rapid analysis of intermediates of Tanreqing injection. *Journal of Pharmaceutical and Biomedical Analysis*, 53(3):350-358, 2010.
- O. Haavisto, H. Hyötyniemi. Recursive multimodel partial least squares estimation of mineral flotation slurry contents using optical reflectance spectra. *Analytica Chimica Acta*, 642(1):102-109, 2009.
- B.S. Dayal, J.F. MacGregor. Improved PLS algorithms. *Journal of Chemometrics*, 11(1):73-85, 1997.
- B.S. Dayal, J.F. MacGregor. Recursive exponentially weighted PLS and its applications to adaptive control and prediction. *Journal of Process Control*, 7(3):169-179, 1997.
- M. Chen. Data-driven methods for near infrared spectroscopy modelling. *MSc Thesis. University of Alberta*, Fall 2013.
- J.D. Hamilton. Rational-expectations econometric analysis of changes in regime - An investigation of the term structure of interest rates. *Journal of Economic Dynamics and Control*, 12(2):385-423, 1988.
- J.D. Hamilton. Analysis of time series subject to changes in regime. *Journal of Econometrics*, 45(1):39-70, 1990.
- N. Sammaknejad, B. Huang, A. Fatehi, Y. Miao, F. Xu, A. Espejo. Adaptive monitoring of the process operation based on symbolic episode representation and hidden Markov models with application toward an oil sand primary separation. *Computers and Chemical Engineering*, 71:281-297, 2014.
- N. Sammaknejad, B. Huang, W. Xiong, A. Fatehi, F. Xu, A. Espejo. Operating condition diagnosis based on HMM with adaptive transition probabilities in presence of missing observations. *AIChE Journal*, 61(2):477-493, 2015.